Numerical Modeling of Large Stretch of Adhesive Fibrils

K. Patel[1], M. Ciccotti [1] , E. Barthel [1]

[1] Laboratoire de Sciences et Ingénierie de la Matière Molle, ESPCI Paris,
Université PSL, Sorbonne Université, CNRS, 75005 Paris, France

Scotch tape and peeling

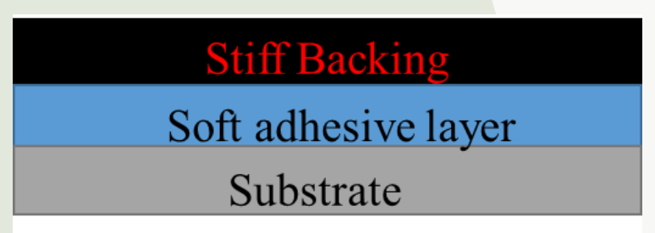

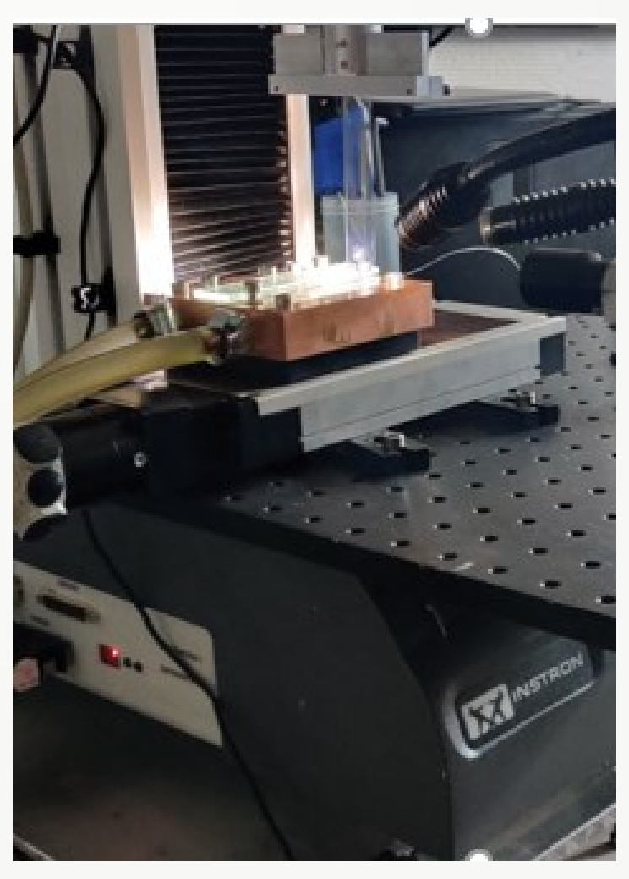

Instrumented Peeling

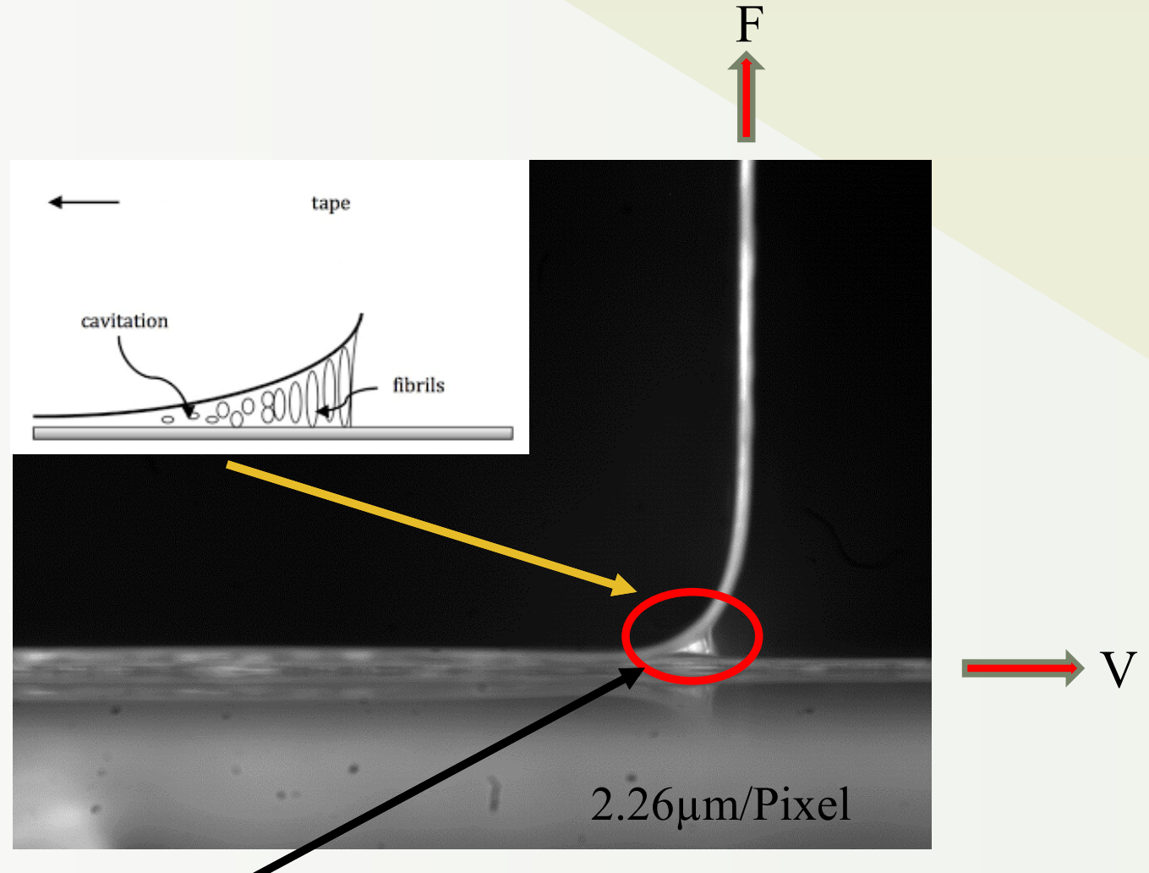

Cohesive zone

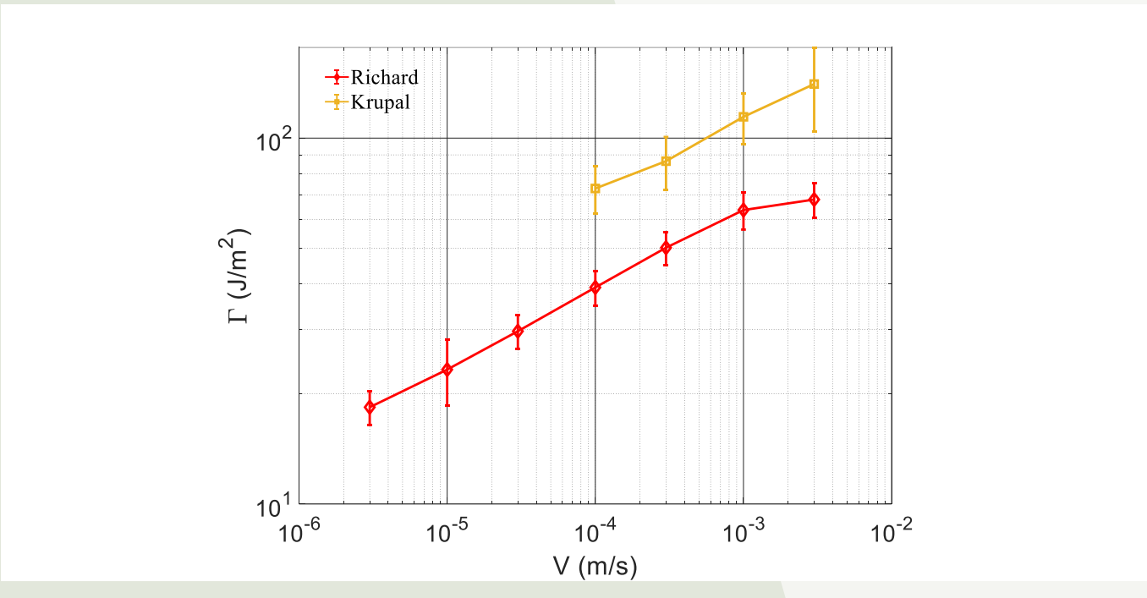

$$\Gamma = \frac{F}{b}$$

b = width of the scotch tape
F= force
Γ = adherence energy
V= velocity

$$\Gamma = a_0 \times \sigma \times \frac{(a_f - a_0)}{a_0}$$

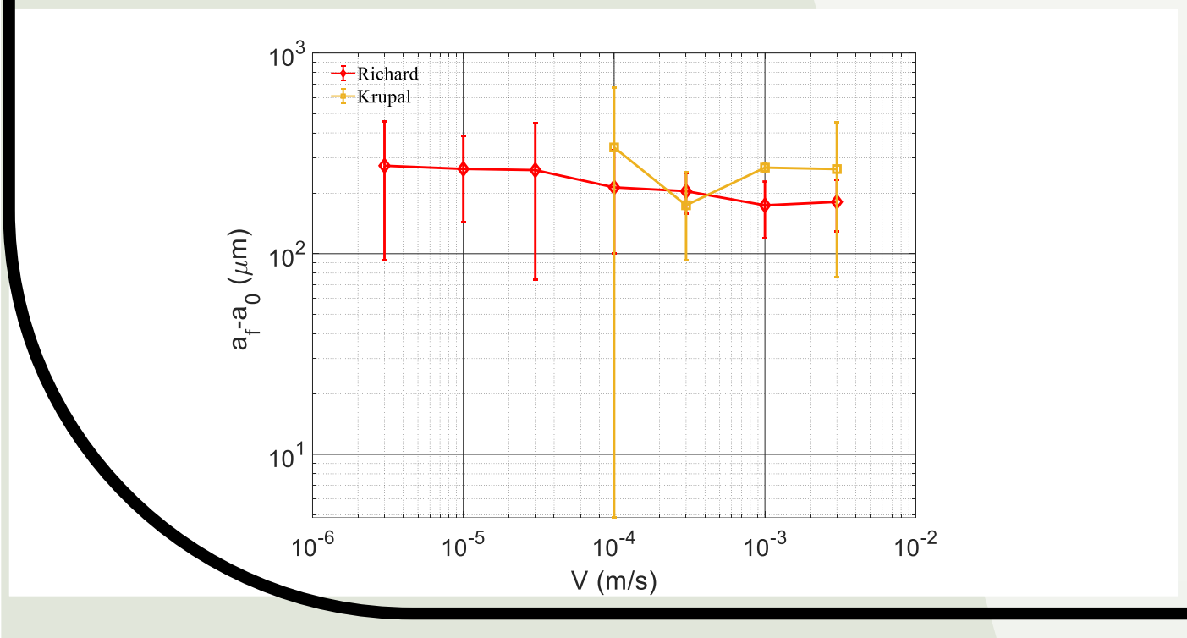

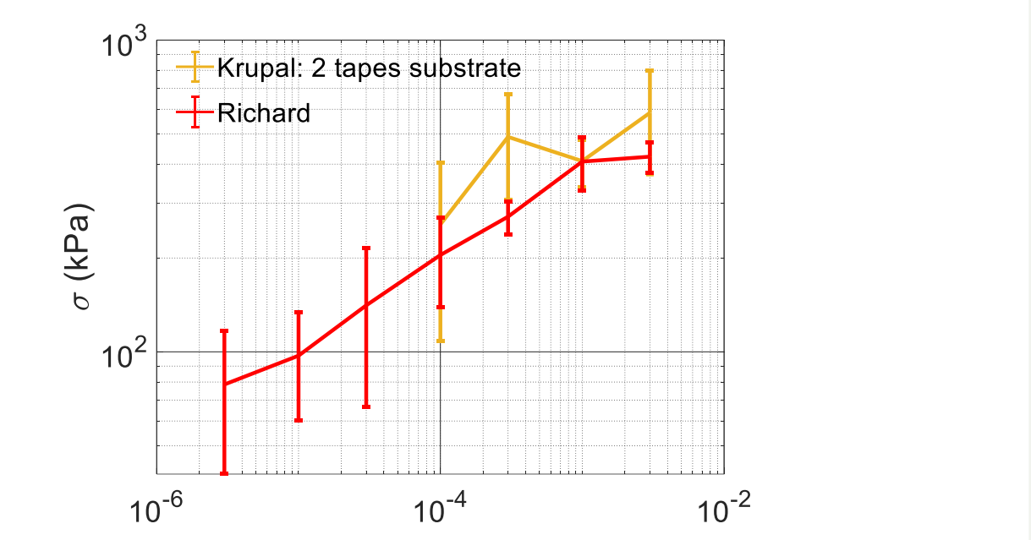

Julien's model for peeling

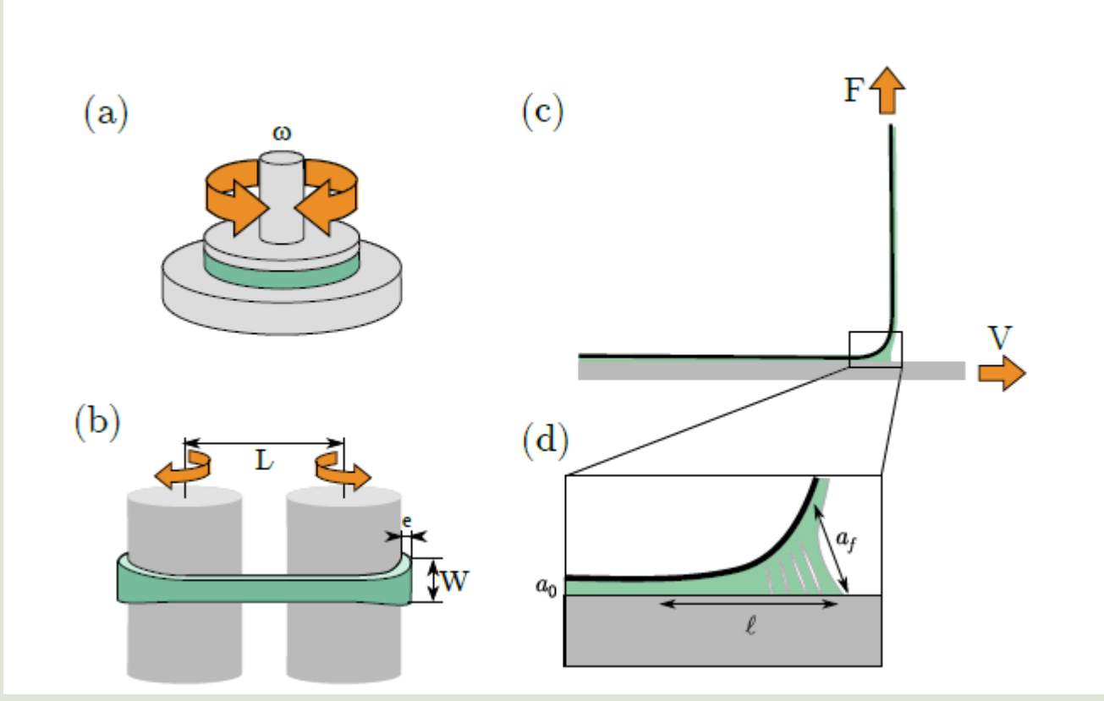

Schematics of experimental setups

Where l =lateral size and a_f = maximal fibril size
For this geometry energy release rate $G = \frac{F}{b}$
The adhesive layer thickness a_0 = 19 µm

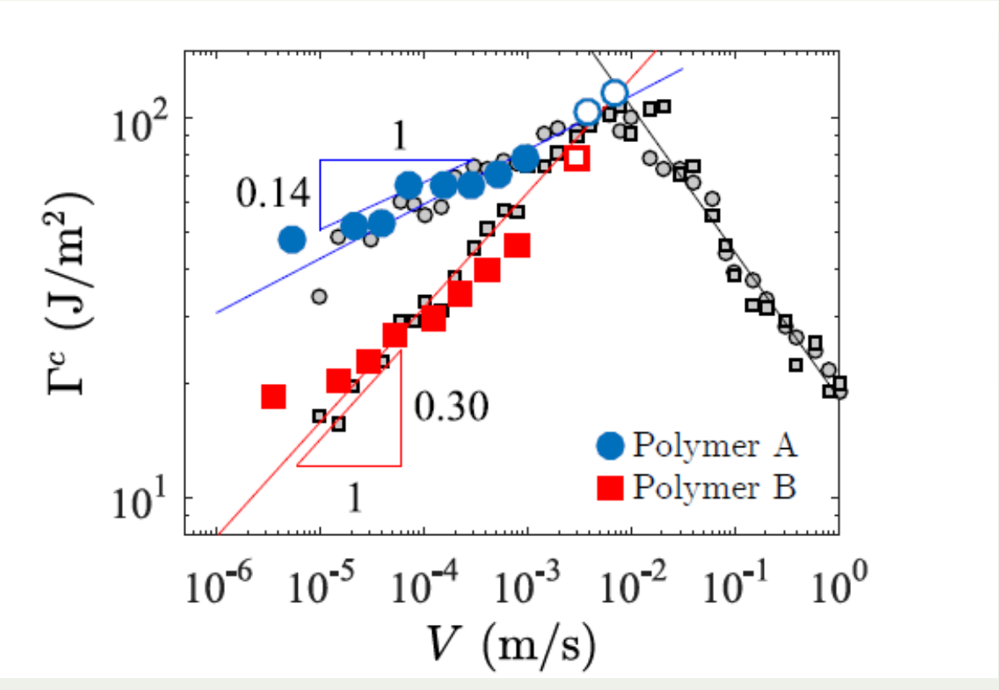

Rupture energy $\Gamma^c(V) = a_0\, k_{exp} \int_0^{\varepsilon_f(\dot{\varepsilon_a})} \sigma(\varepsilon', \dot{\varepsilon_a})\, d\varepsilon'$

- The dimensionless prefactor k_{exp}, can be interpreted as the sign that the fibril drawing process from the bulk adhesive layer is affected by a higher stress triaxiality.
- Value of prefactor: k_{exp}=5.

Constitutive Relations

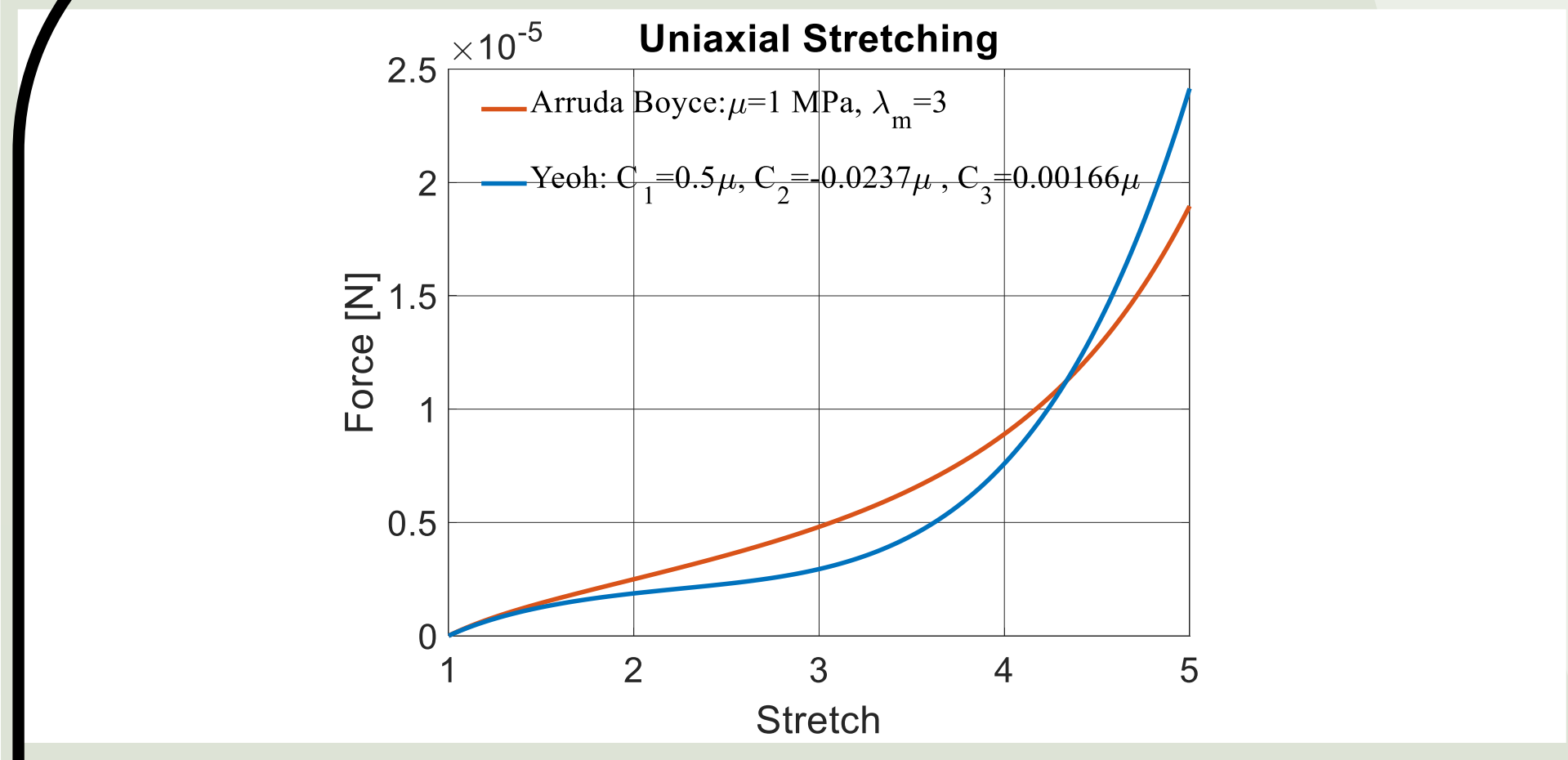

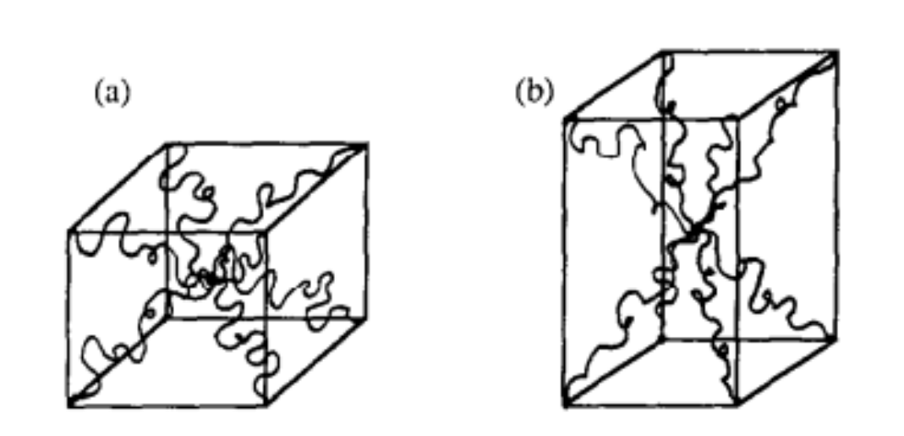

Eight chain model for (a) undeformed and (b) uniaxial extension configuration

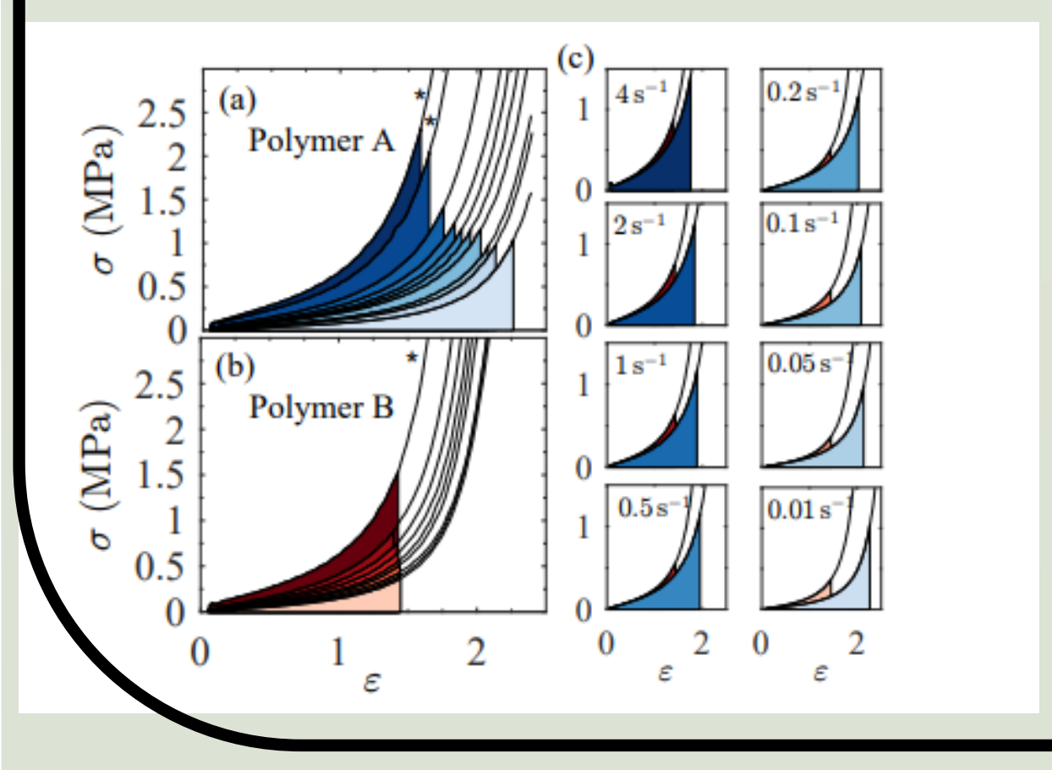

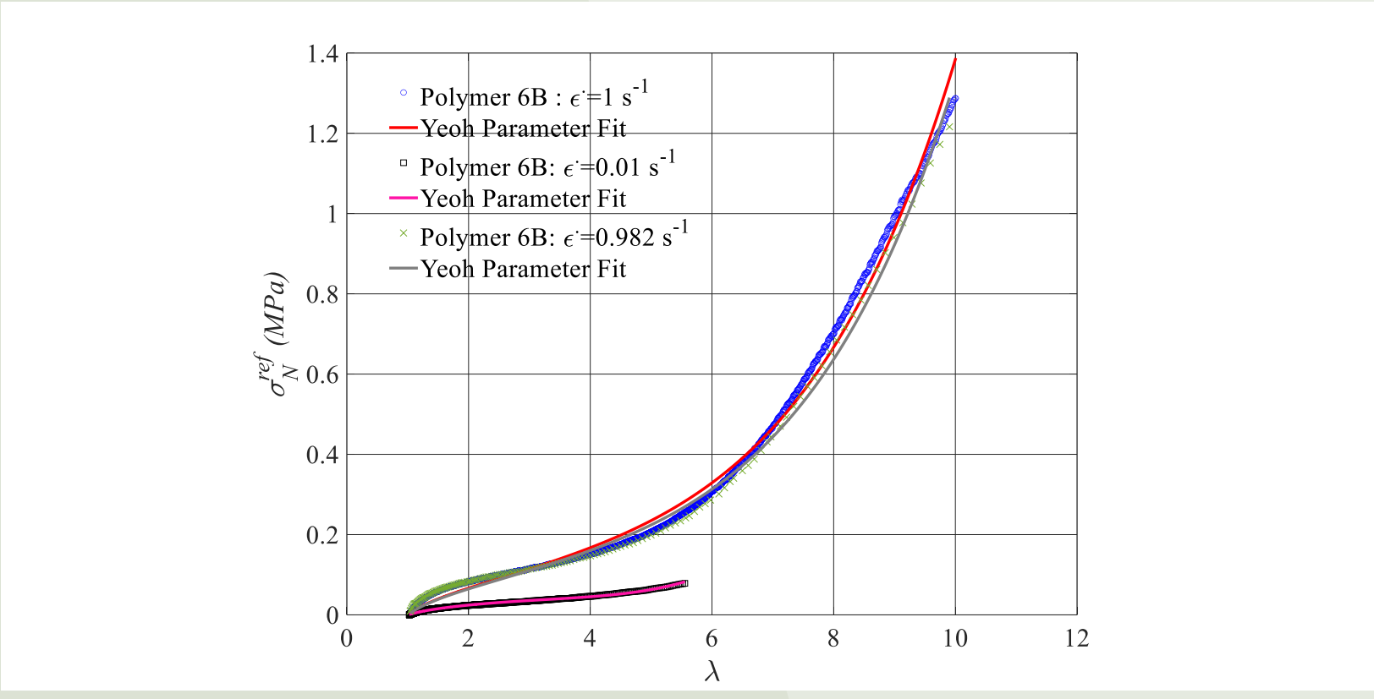

FEM Implementation of modeling single fibril

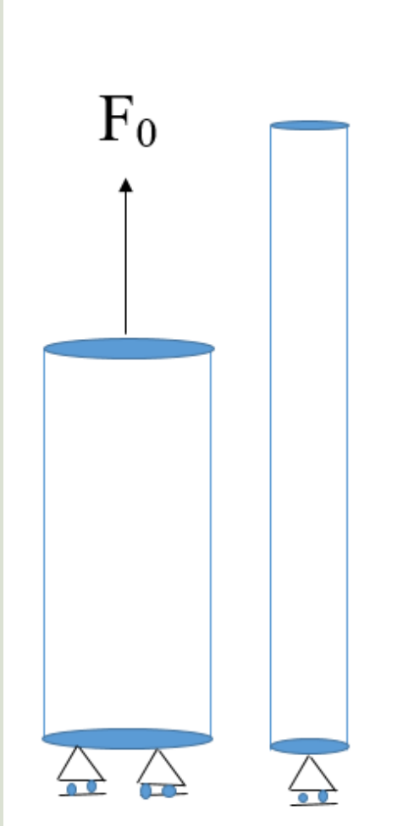

Uniaxial Extension

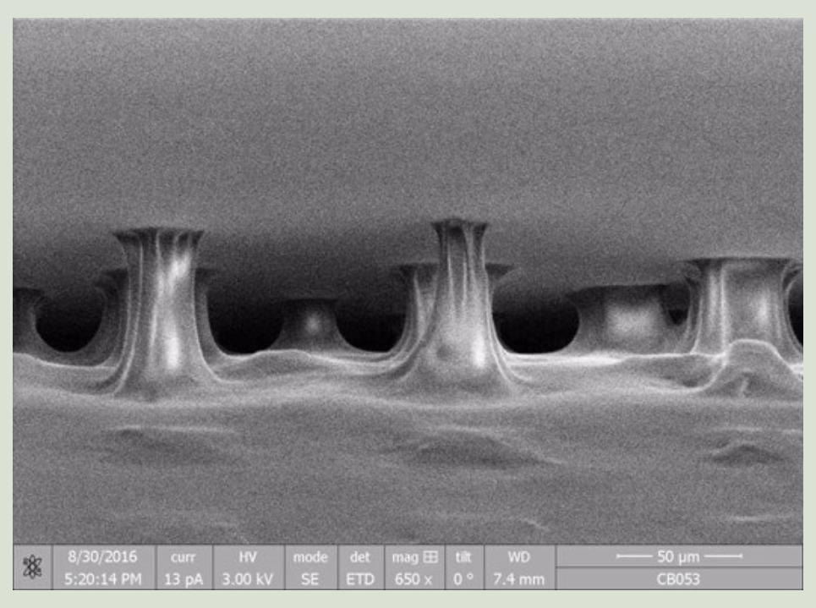

SEM view of adhesion rupture of a PSA tape, showing fibrillation (X. Morelle & B. Bresson)

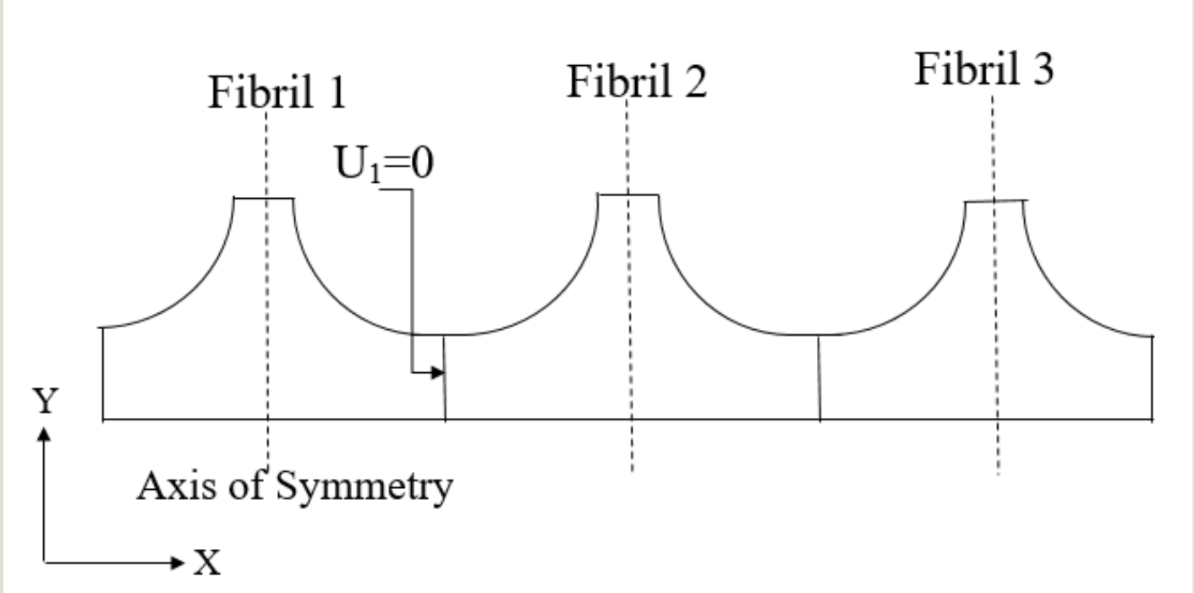

Schematics of the fibrils in PSA

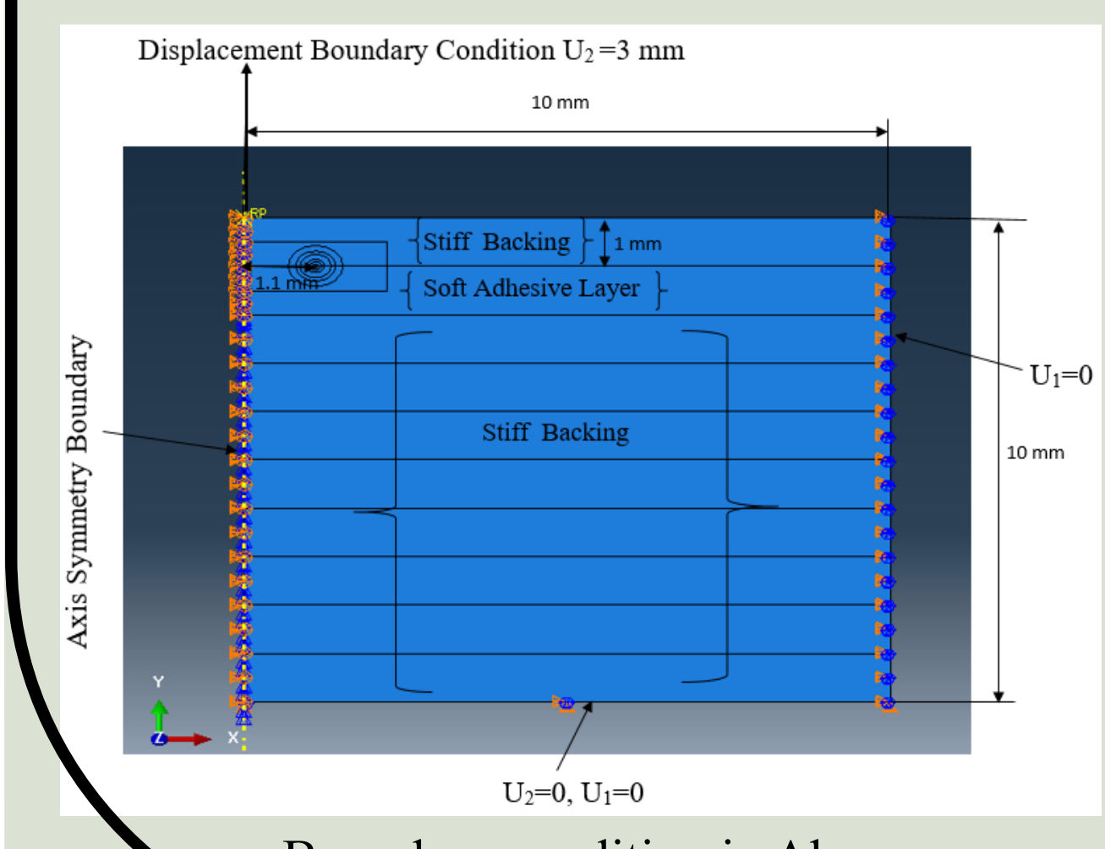

Boundary condition in Abaqus

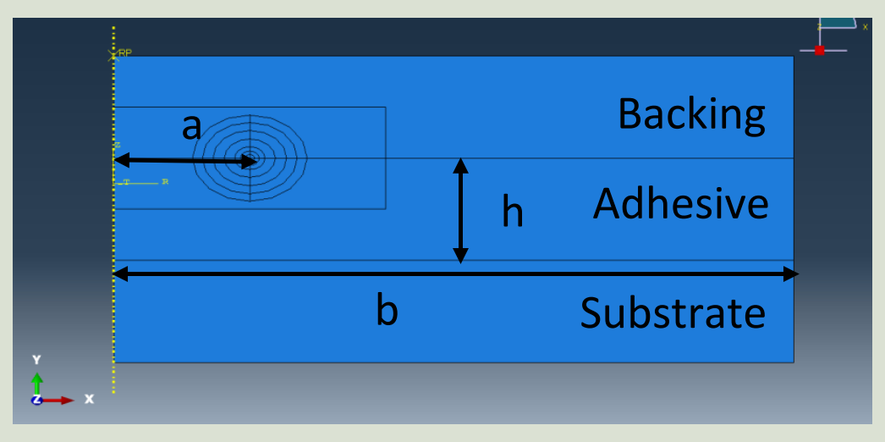

Initial configuration of the fibril

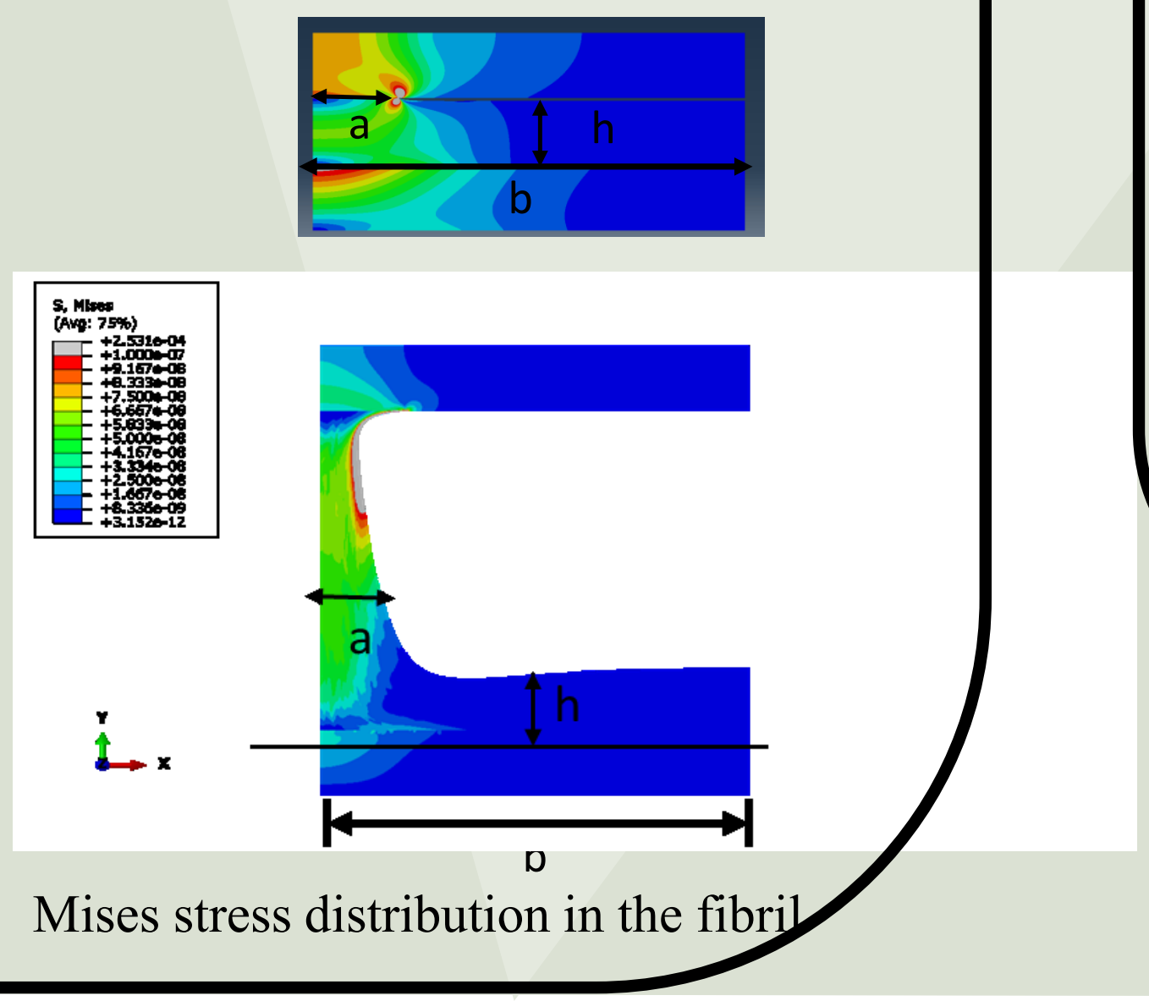

Mises stress distribution in the fibril

$$\Gamma^c(V) = a_0\, k_{exp} \int_0^{\varepsilon_f(\dot{\varepsilon_a})} \sigma(\varepsilon', \dot{\varepsilon_a})\, d\varepsilon'$$

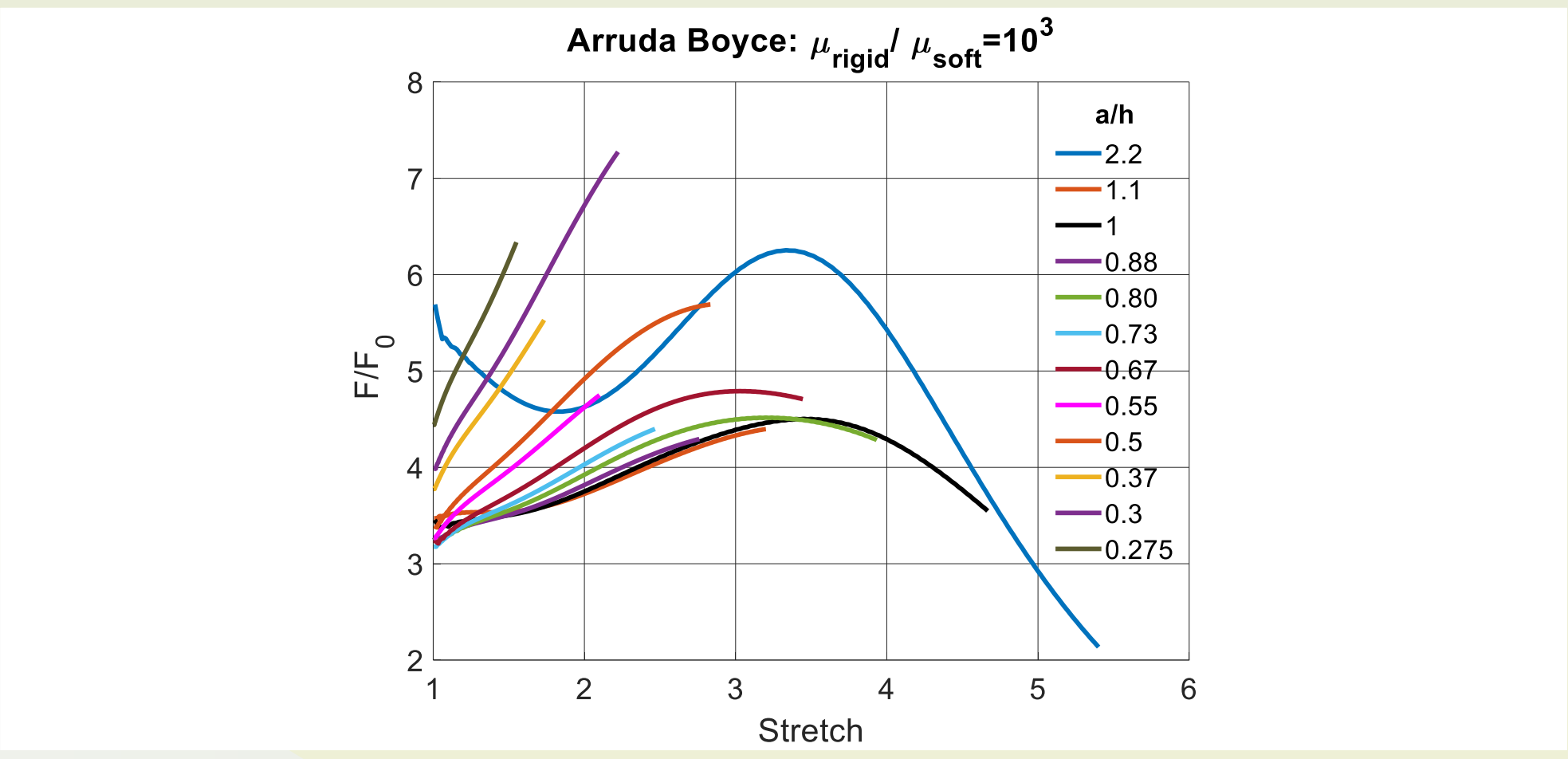

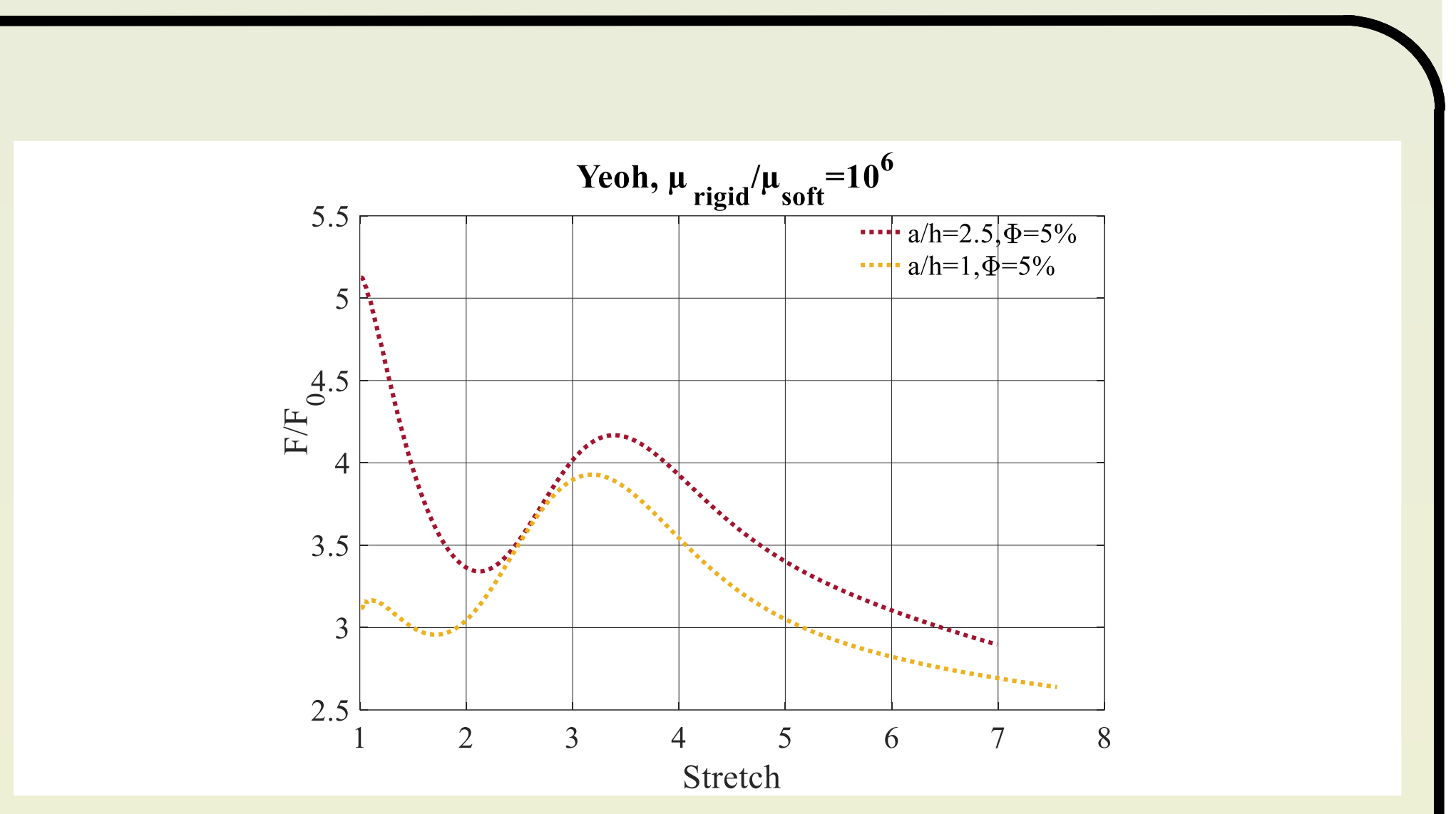

Where, F= force in fibril simulation and F_0= force in uniaxial simulation for the same stretch , a= radius of the fibril and h= thickness of the soft layer

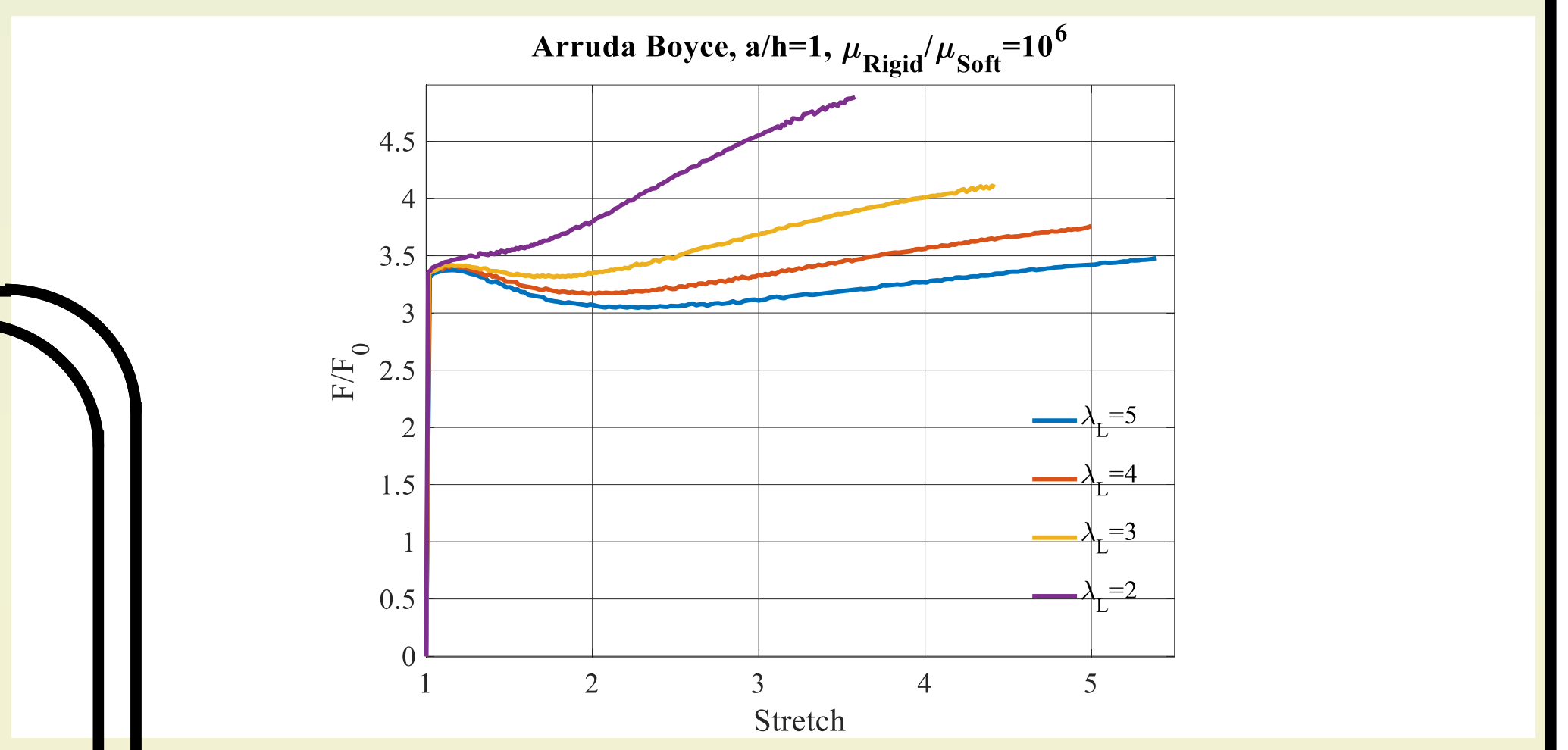

Simulated Fibril vs Experimental Fibril

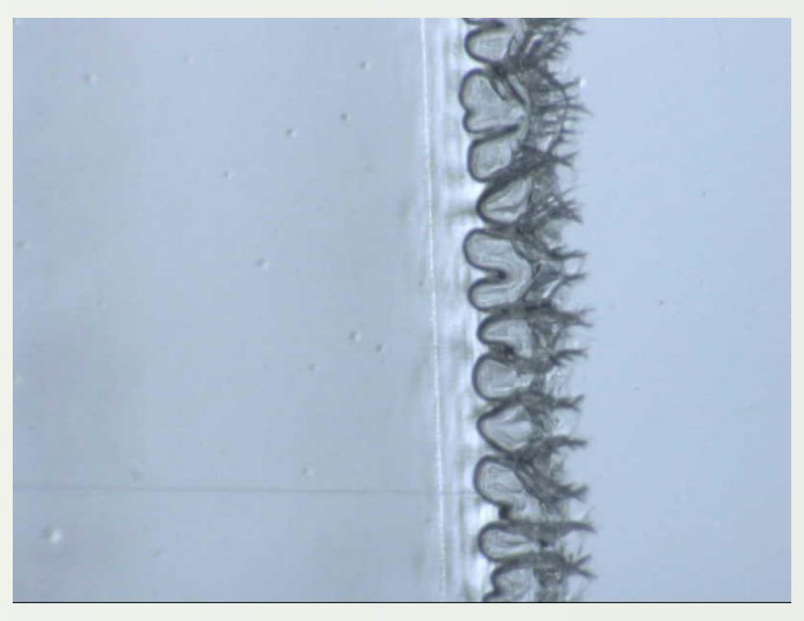

Peeling front from bottom on homogeneous substrate

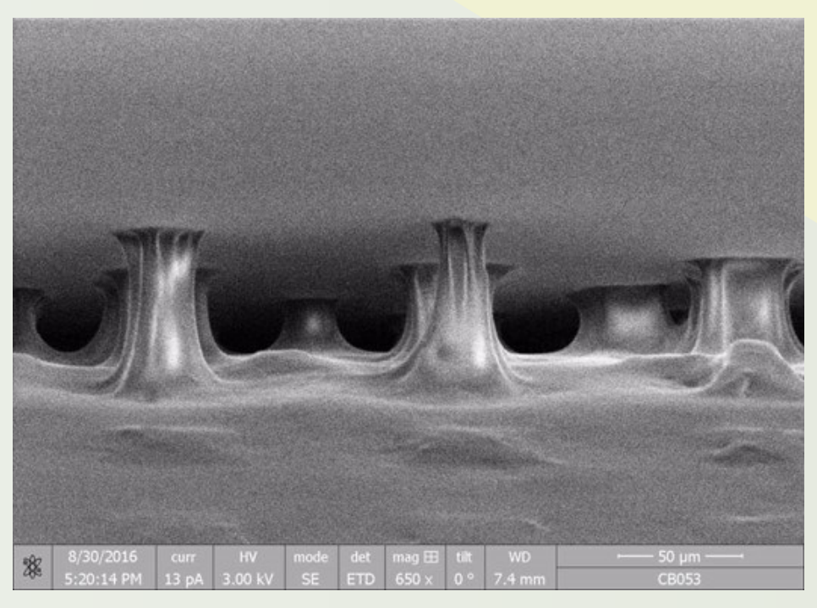

SEM view of adhesion rupture of a PSA tape, showing fibrillation (X. Morelle & B. Bresson)

Yeoh model
a/h=2.5
Φ =5%
µ=55kPa
Stretch λ = 4
$\dot{\lambda}$ = 3.3 s^{-1}
Peeling velocity
V=0.1mm/s
Polymer 6B

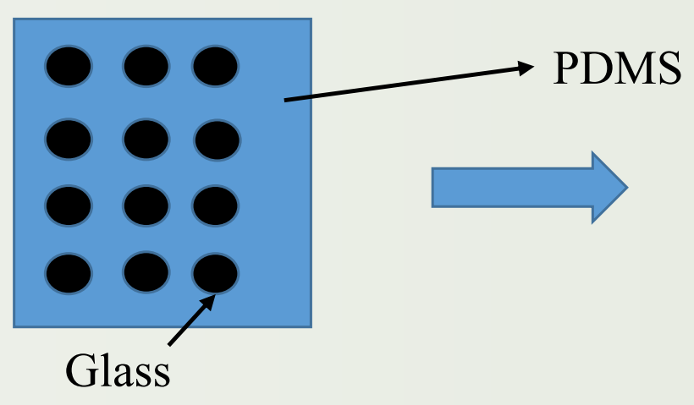

E_{fib} = 2µJ/ fibril

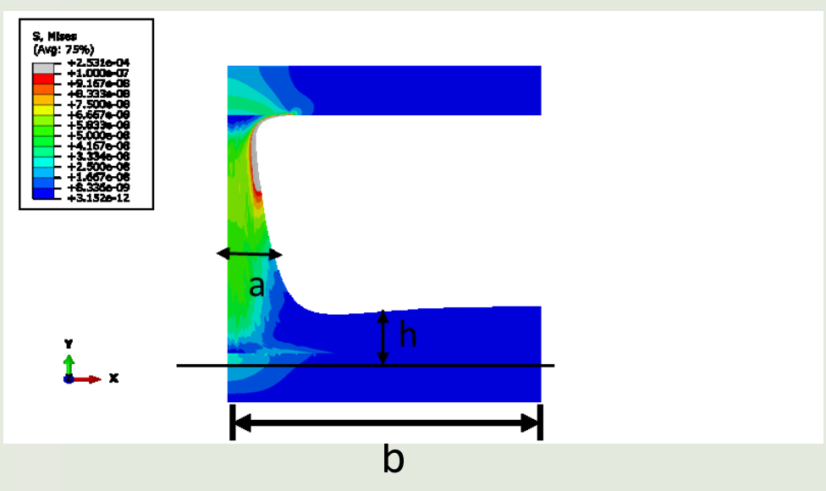

E_{fib} = 0.168 µJ/ fibril

Validation: Small strain calculations

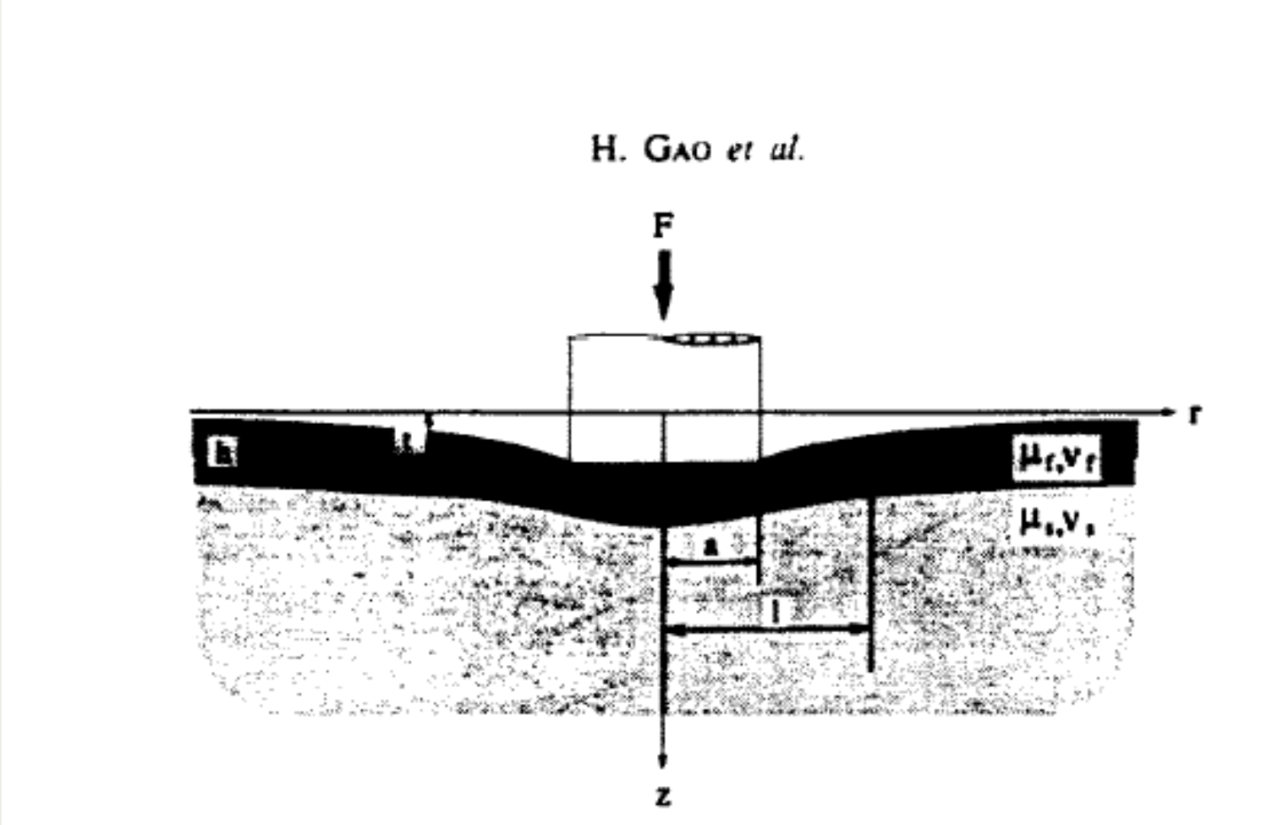

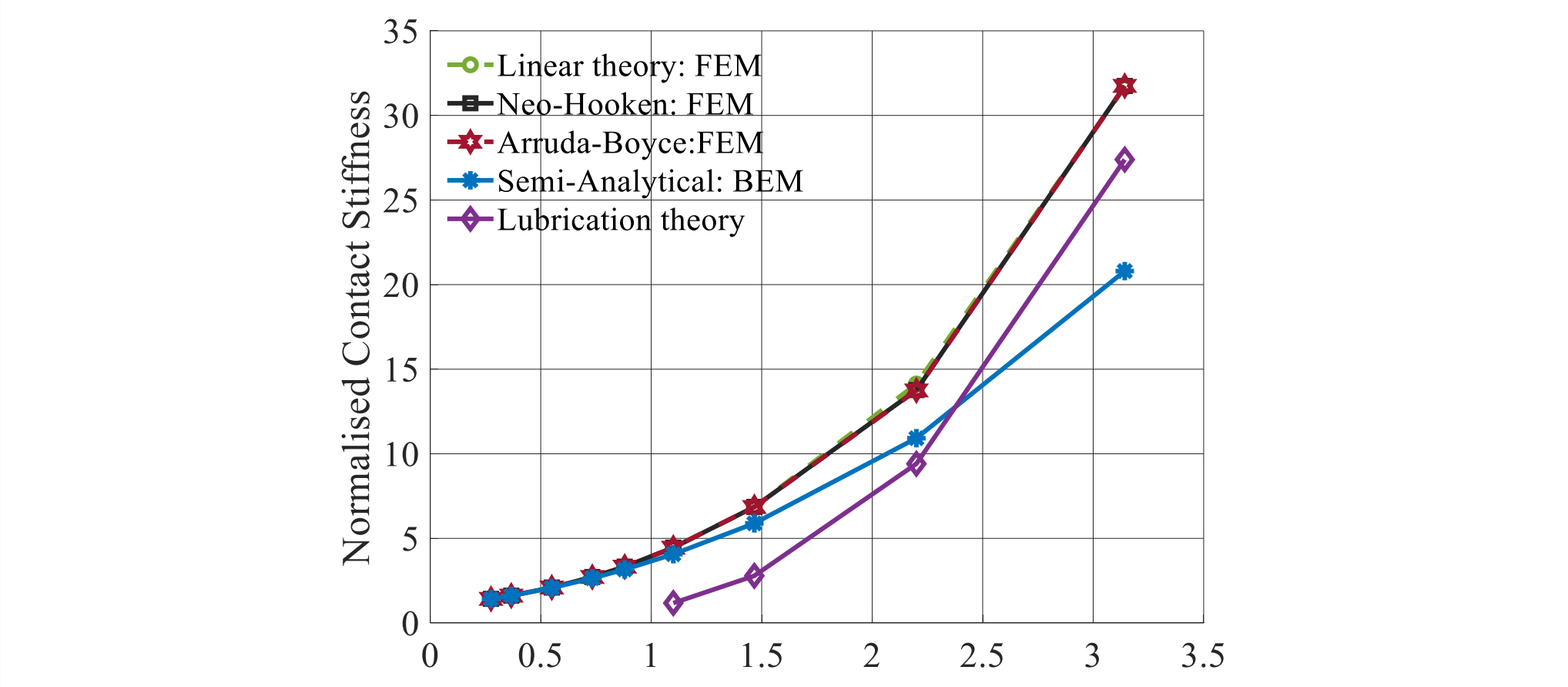

Cavitation

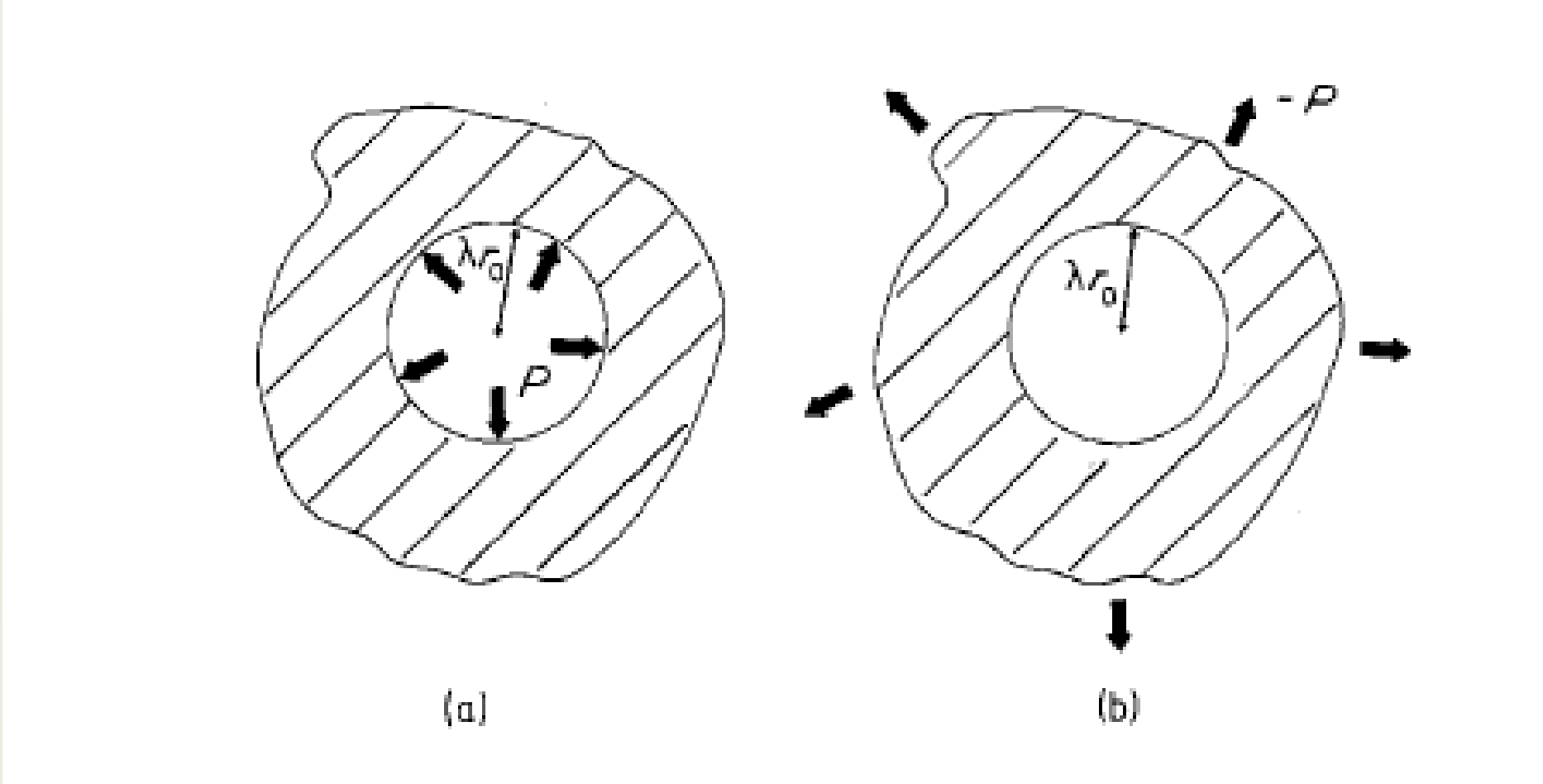

Figure 1 (a) Sketch of an inflated spherical void; (b) spherical void in a medium under a far-field triaxial tension (negative pressure) of $-P$.

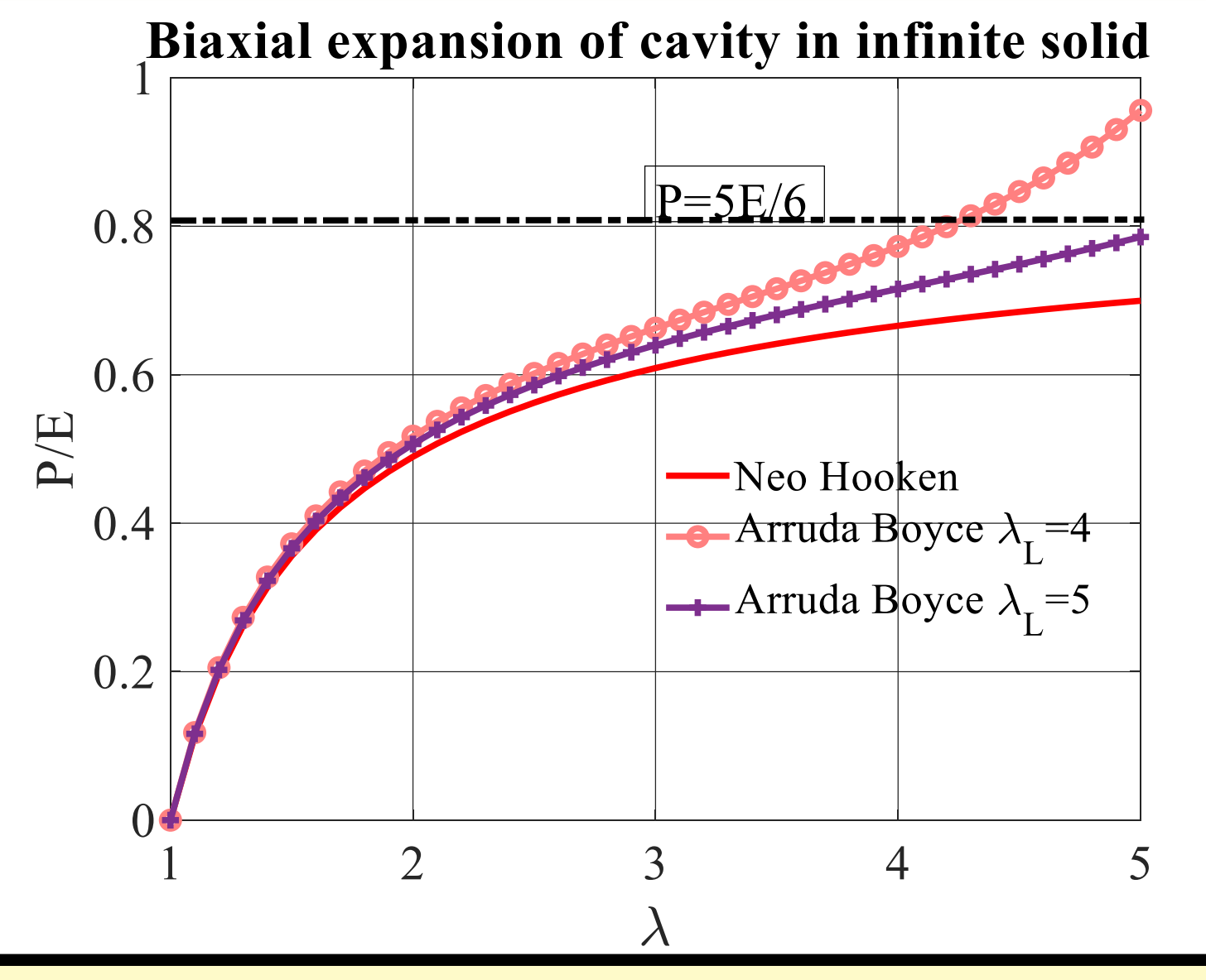

$$\frac{P}{E} = \frac{(5 - 4\lambda^{-1} - \lambda^{-4})}{6}$$

Conclusions

- At small strain, fibril simulation predicts the factor of 3.3 ($k_{simulation}$=F/F_0) for a/h=1.1,1
- This factor comes from the confinement between the backing and the substrate
- Small strain validation of the fibril simulation is in good agreement with the available semi analytical results for moduli mismatch ratio of 100
- Matching simulated fibril energy with experimental debonding energy on patterned substrate require accounting for PDMS contribution
- However, cavitation can be included in the simulation to check whether initial configuration has any role to play in the over all results.
- Cavities in the infinite solid expand without any limit at critical pressure for Neo-Hooken solid. But, if we consider strain hardening and use Arruda-Boyce model than this is not true.

References

- *A three-dimensional constitutive model for large stretch behavior of rubber elastic materials; Journal of the Mechanics and Physics of Solids*; Elsevier; 1993;41 (2),pp.389-412 ; Ellen M. Arruda, Mary C. Boyce
- *Nonlinear Viscoelastic Modeling of Adhesive Failure for Polyacrylate Pressure-sensitive Adhesives; Macromolecules;2018; 51 (21); 8605-8610* ; J. Chopin et. al
- *Elastic contact vs indentation modeling of multilayered materials*; *Int. J. of solids structures; 1992;* H. Gao et al.
- *Adhesive elastic contacts: JKR and more; J. Phys. D: Appl. Phys.; 2008; 41 163001 (20pp);* E. Barthel
- *Elastic contact to a coated half-space - effective elastic modulus and real penetration; Journal of Material Research; 2004; 19:600–608;* A. Perriot and E. Barthel
- *Fracture mechanics and cavitation in rubber-like solids. Journal of Materials Science; 1991; 23:3392–3395;* A.N. Gent and C. Wang

Acknowledgement

This project has received funding from the European Union's Horizon 2020 research and innovation programme under the Marie Skłodowska-Curie grant agreement No 754387